自旋電子學簡介
Introduction to Spintronics

奈米磁性材料製作與分析
Fabrication and analysis of magnetic nanostructures

李　尚　凡
中央研究院　物理所

- 磁性材料 巨磁阻 GMR 穿隧磁阻 TMR
- 全金屬 自旋電晶體 Spin transistor
- 磁性 金屬自旋閥 半導體電晶體 Spin-valve transistor
- 磁性半導體 Dilute magnetic semiconductors
- 極化電流推動磁區壁 Magnetization reversal by spin-polarized current

鐵磁性元素：鐵, 鈷, 鎳, 釓, 鏑, 錳, 鈀

Elements with ferromagnetic properties

合金, alloys

錳氧化物 MnOx

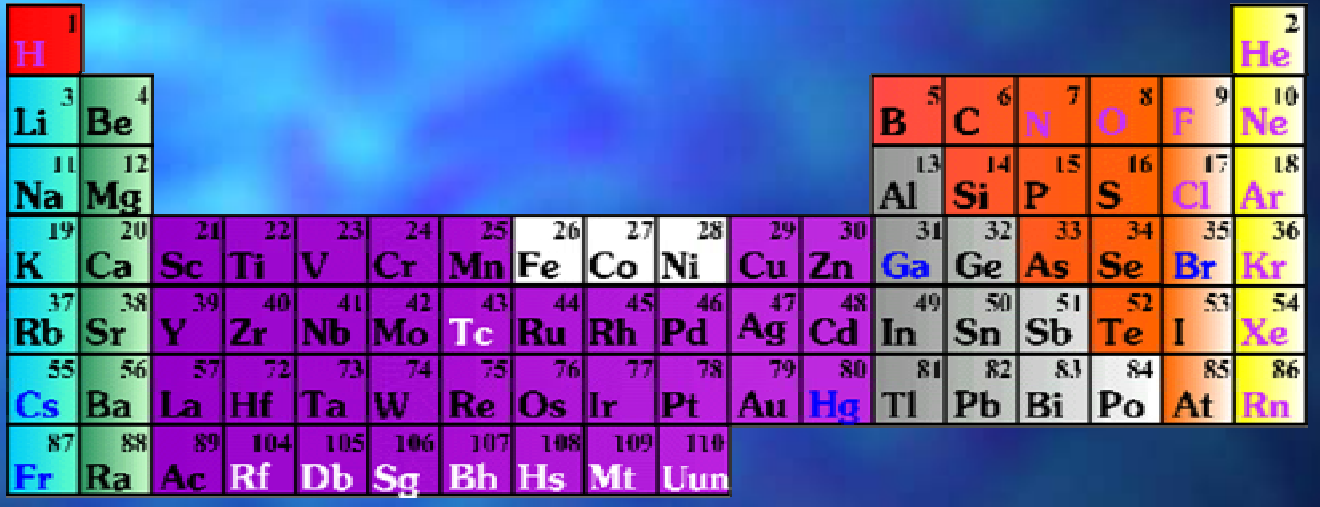

電子帶有自旋,一般物質中自旋向上與向下的電子數目相等,鐵磁性物質在居禮溫度以下,兩者不相等.

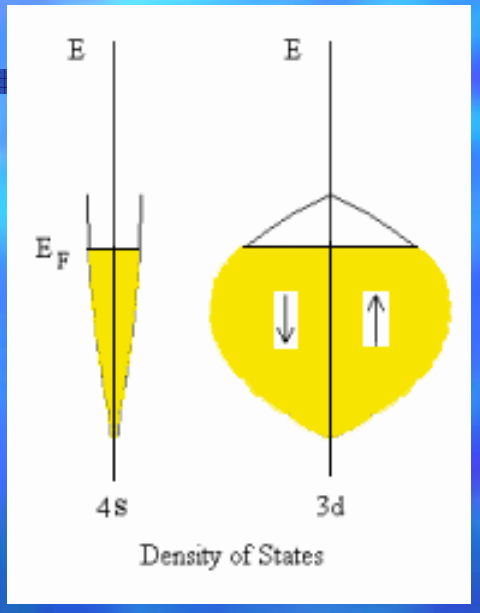

銅

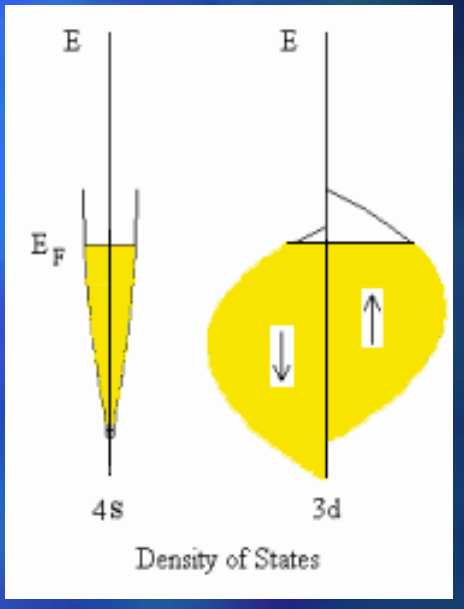

鈷

晶體上層電子能態示意圖. 自旋向上與向下電子總數不同,造成物質帶有磁性. 費米面附近電子數及空的能態數不同,則造成了傳導電子偏極化.

Particle's energy

$$E = V_m \{ K \sin^2\theta + H M_s \cos\theta \}$$

$$\frac{\partial E}{\partial \theta} = V_m \{ 2K \sin\theta\cos\theta - H M_s \sin\theta \}$$

$$= 0,$$

$$\Rightarrow (2K\cos\theta - H M_s)\sin\theta = 0$$

① $\sin\theta = 0$, $\theta = 0, \pi$

② $\cos\theta = \frac{H M_s}{2K}$

ΔE ($\cos\theta = \frac{H M_s}{2K}$, $\theta = 0$) =

$$E(\theta = 0) = V_m H M_s$$

$$E\left(\cos\theta = \frac{H M_s}{2K}\right) = V_m \left\{ K \sin^2\theta + \frac{H^2 M_s^2}{2K} \right\}$$

$$= V_m \left\{ K \left[1 - \left(\frac{H M_s}{2K} \right)^2 \right] + \frac{H^2 M_s^2}{2K} \right\}$$

$$= V_m \left\{ K - \frac{H^2 M_s^2}{4K} + \frac{H^2 M_s^2}{2K} \right\}$$

$$= V_m K \left\{ 1 + \left(\frac{H M_s}{2K} \right)^2 \right\}$$

$\theta = 0, \pi$ $\Delta E = V_m K \left\{ 1 - \frac{H M_s}{K} + \left(\frac{H M_s}{2K} \right)^2 \right\}$

$$= V_m K \left\{ 1 - \frac{H M_s}{2K} \right\}^2$$

$k_B T \Leftrightarrow \Delta E$

$\tau = \tau_0 \exp\left(\frac{KV}{k_B T} \right)$ $\tau_0 \sim 10^{-9} \sim 10^{-13}$ sec

$\tau_m \sim 1 \sim 100$ sec.

$\ln\left(\frac{\tau_m}{\tau_0}\right) = \frac{KV}{k_B T}$ $T_B = \frac{KV}{k_B \ln\frac{\tau_m}{\tau_0}}$ $\ln\frac{\tau_m}{\tau_0} \sim 25$

$\Rightarrow V_p \sim \frac{25 k_B T}{K}$

研究院物理研究所

$$\langle X \rangle = M_s L(X) \qquad L(X) = \coth(X) - \frac{1}{X}$$

$$X = \frac{\mu_{cluster}(H + \lambda M)}{k_B T}$$

$$\mu_{cluster} = \mu_{atom} N = M_s V$$

vector theory

uniformly distributed unit vectors on a sphere when H is

$$U = -MH\cos\theta$$

probability of spin in H direction is $\propto$ Boltzmann

$$\exp\left(-\frac{U}{k_B T}\right) = \exp\left(\frac{MH}{k_B T}\cos\theta\right)$$

$$p(\theta)\,d\theta = \frac{\exp\left(\frac{MH}{k_B T}\cos\theta\right)\sin\theta\,d\theta}{\int_0^{\pi} \exp\left(\frac{MH}{k_B T}\cos\theta\right)\sin\theta\,d\theta}$$

Magnetization $I = NM\,\overline{\cos\theta} = NM\int_0^{\pi}\cos\theta\, p(\theta)\,d\theta$

$$\frac{MH}{k_B T} = \alpha \qquad \cos\theta = x \qquad -\sin\theta\,d\theta = dx$$

$$I = NM\,\frac{\int_{-1}^{1} e^{\alpha x} x\,dx}{\int_{-1}^{1} e^{\alpha x}\,dx} \qquad \int_{-1}^{1} e^{\alpha x} x\,dx = \frac{1}{\alpha}\left(e^{\alpha} + e^{-\alpha}\right) - \frac{1}{\alpha^2}\left(e^{\alpha} - e^{-\alpha}\right)$$

$$\int_{-1}^{1} e^{\alpha x}\,dx = \frac{1}{\alpha}\left|e^{\alpha x}\right|_{-1}^{1} = \frac{1}{\alpha}\left(e^{\alpha} - e^{-\alpha}\right)$$

$$= NM\left(\coth\alpha - \frac{1}{\alpha}\right)$$

- Anisotropic Magnetoresistance
- GMR Giant Magnetoresistance
- CMR Colossal Magnetoresistance
- Tunneling Magnetoresistance
- Ballistic Magnetoresistance

異向磁阻 (Anisotropic Magnetoresistance)
巨磁阻(Giant MR)
龐磁阻(Colossal MR)
穿隧磁阻(Tunneling MR)

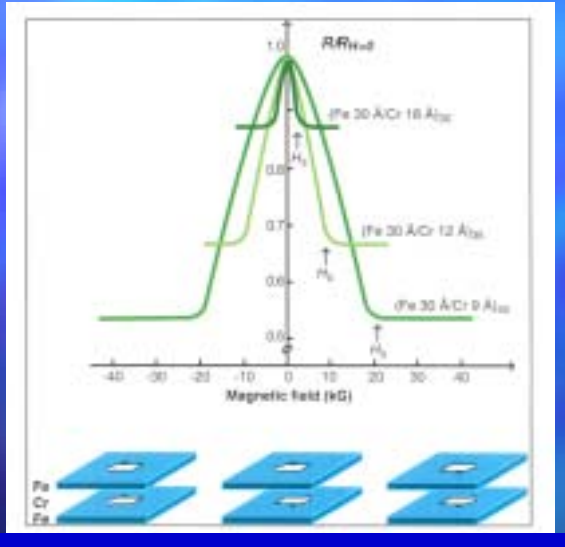

1988 年是磁性傳輸現象史上的里程碑

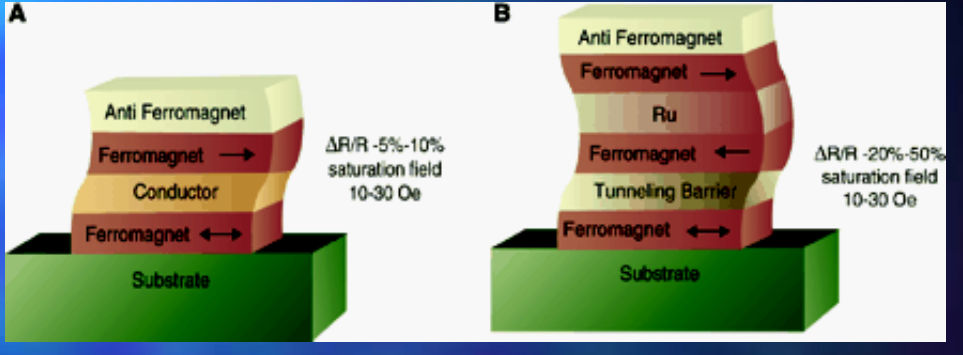

Spin-dependent transport structures. (A) Spin valve. (B) Magnetic tunnel junction.

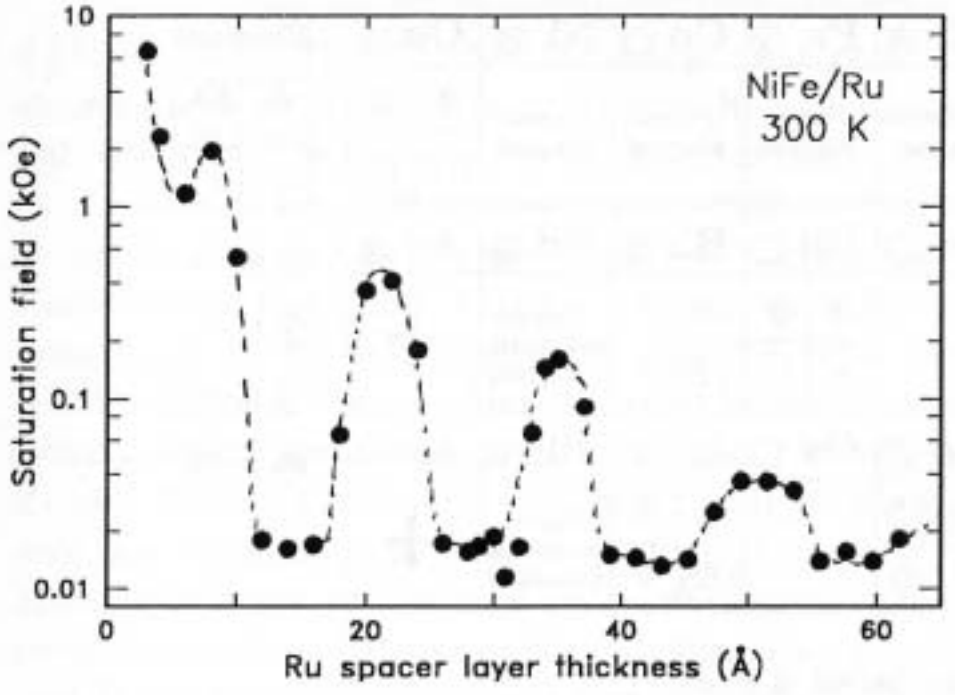

Fig. 2.58. Dependence of saturation field on Ru spacer layer thickness for several series of $Ni_{81}Fe_{19}$/Ru multilayers with structure, 100 Å Ru/[30 Å $Ni_{81}Fe_{19}$/Ru(t_{Ru})]$_{20}$, where the topmost Ru layer thickness is adjusted to be $\simeq$25 Å for all samples

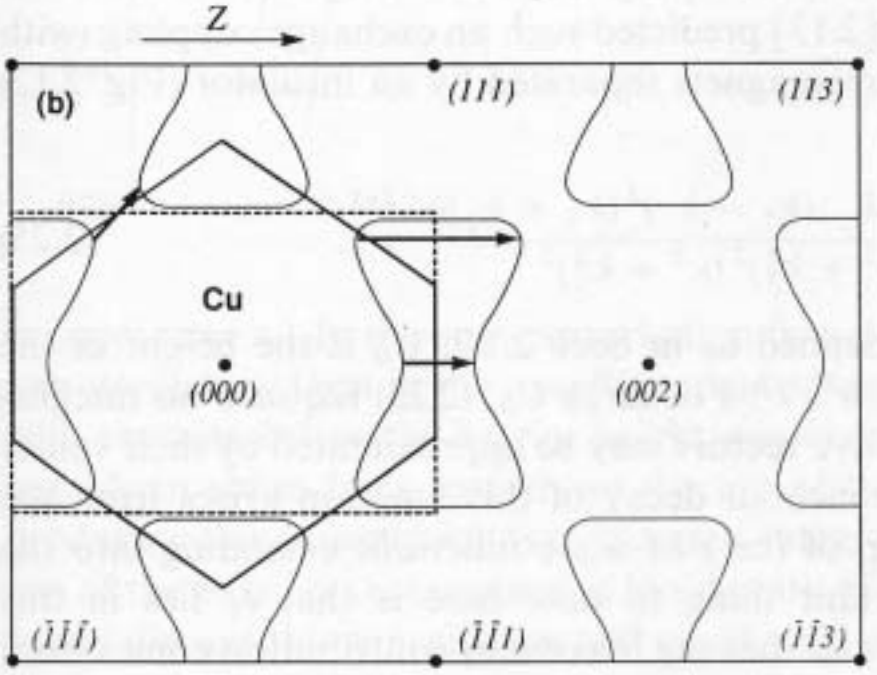

Fig. 2.11. Fermi surface of Cu in the (1 0 0) plane in the extended zone scheme. Arrows indicate values of $2(k_F - G)$ for reciprocal lattice vectors G which can give rise to oscillations with periods greater than π/k_F

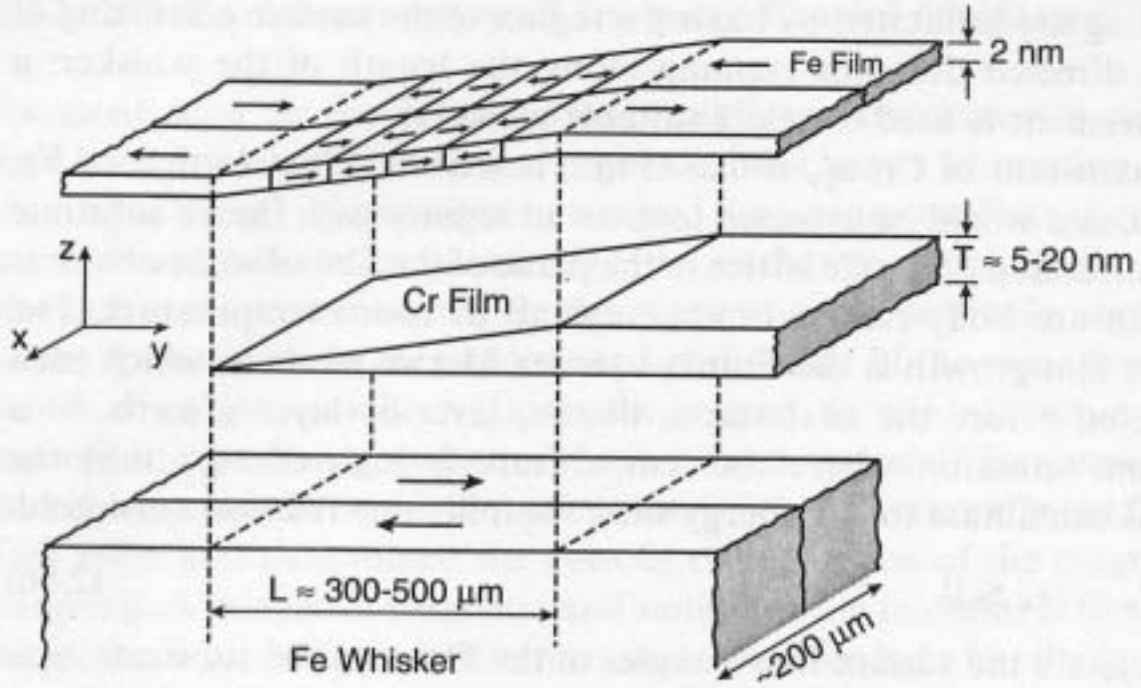

Fig. 2.41. A schematic expanded view of the sample structure showing the Fe(0 0 1) single-crystal whisker substrate, the evaporated Cr wedge, and the Fe overlayer. The arrows in the Fe show the magnetization direction in each domain. The *z*-scale is expanded approximately 5000 times. (From [2.206])

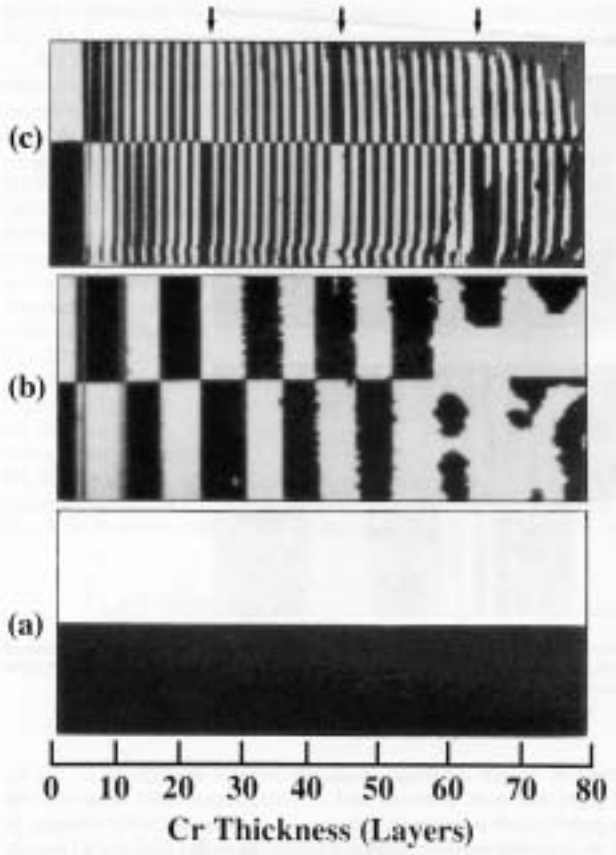

Fig. 2.43. SEMPA image of the magnetization M_x (axes as in Fig. 2.41) showing domains in (a) the clean Fe whisker, (b) the Fe layer covering the Cr spacer layer evaporated at 30 °C, and (c) the Fe layer covering a Cr spacer evaporated on the Fe whisker held at 350 °C. The scale at the bottom shows the increase in the thickness of the Cr wedge in (b) and (c). The arrows at the top of (c) indicate the Cr thicknesses where there are phase slips. The region of the whisker imaged is about 0.5 mm long

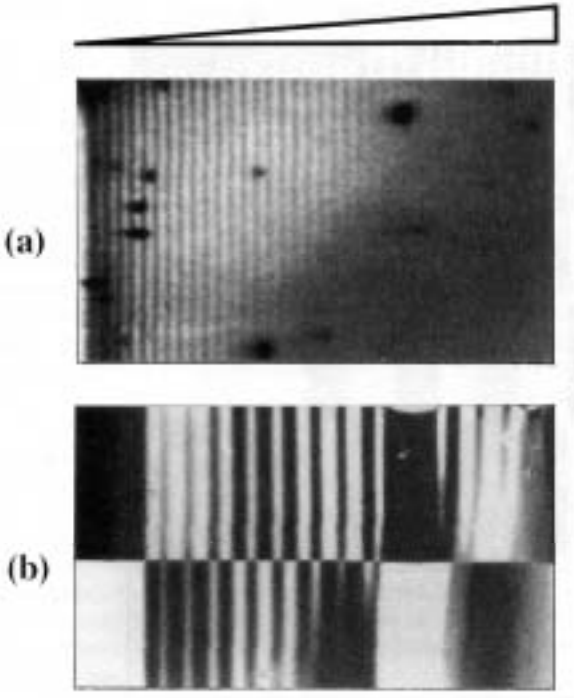

Fig. 2.44. The effect of roughness on the interlayer exchange coupling is shown by a comparison of (a) the oscillations of the RHEED intensity along the bare Cr wedge with (b) the SEMPA magnetization image over the same part of the wedge

Aliasing

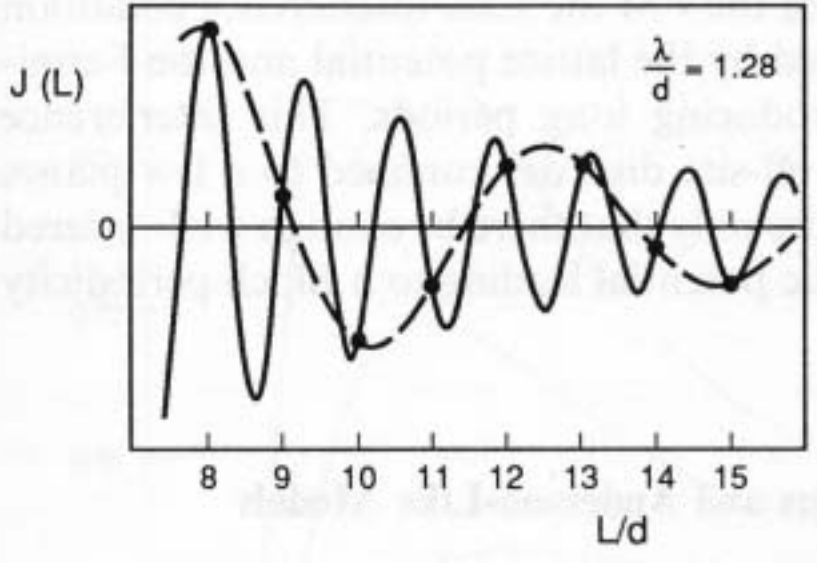

Fig. 2.10. RKKY-like oscillating exchange coupling with period λ (solid line) showing the longer period oscillation (dashed line) obtained by sampling the function only at integral values of the spacing, a, between atomic planes, i.e. "aliasing". From [2.21]

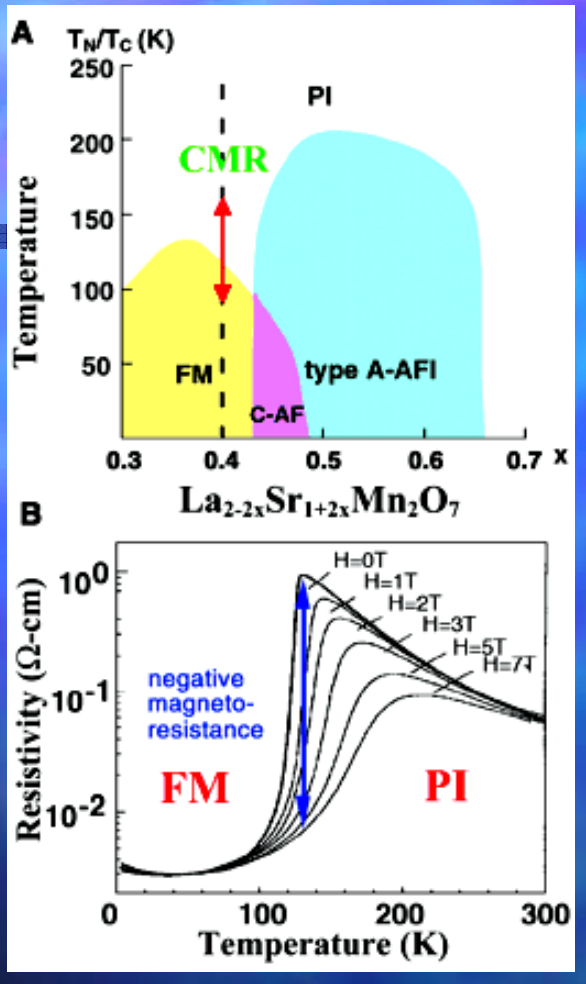

(A) Doping phase diagram for $La_{2-2x}Sr_{1+2x}Mn_2O_7$, extracted from Ling et al. (2). (B) Resistivity versus temperature curves for $La_{1.2}Sr_{1.8}Mn_2O_7$ at various magnetic fields, after Moritomo et al. Nature 380, 141 (1996)

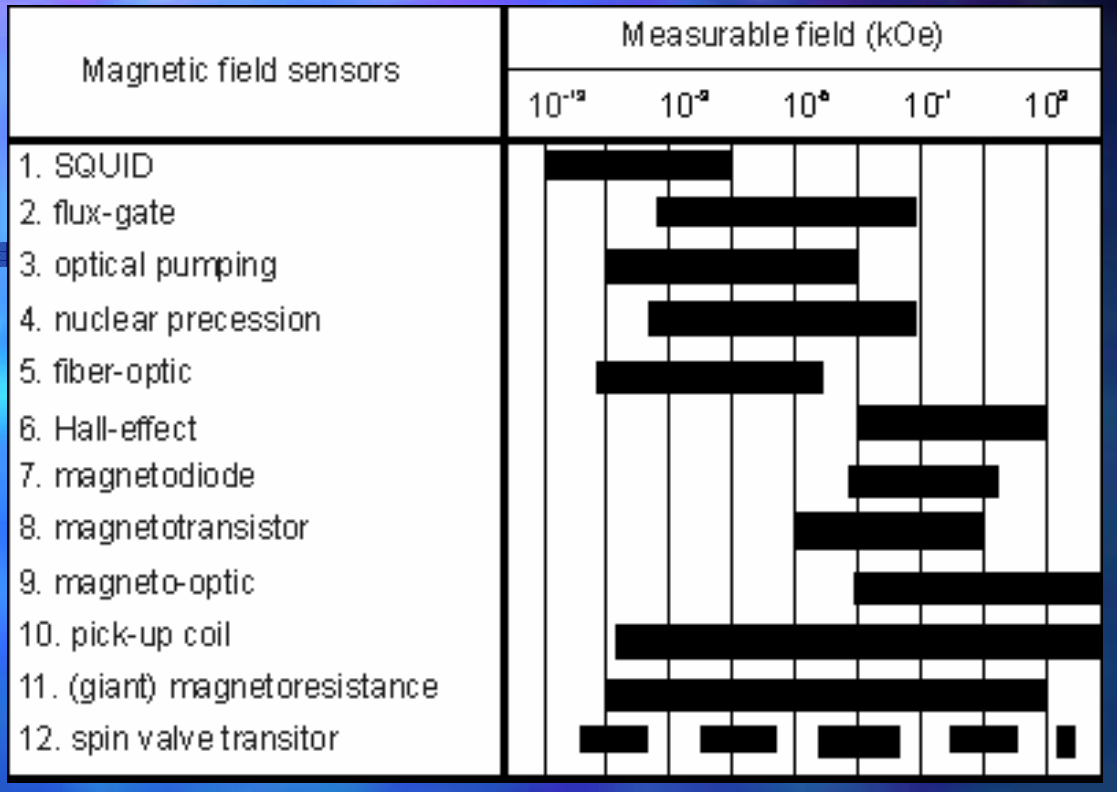

A large variety of magnetic field sensor principles is available. Of major interest is the recently discovered spin valve effect, appearing in an increasing number of varieties. High density recording is a major application of the spin-valve effect.

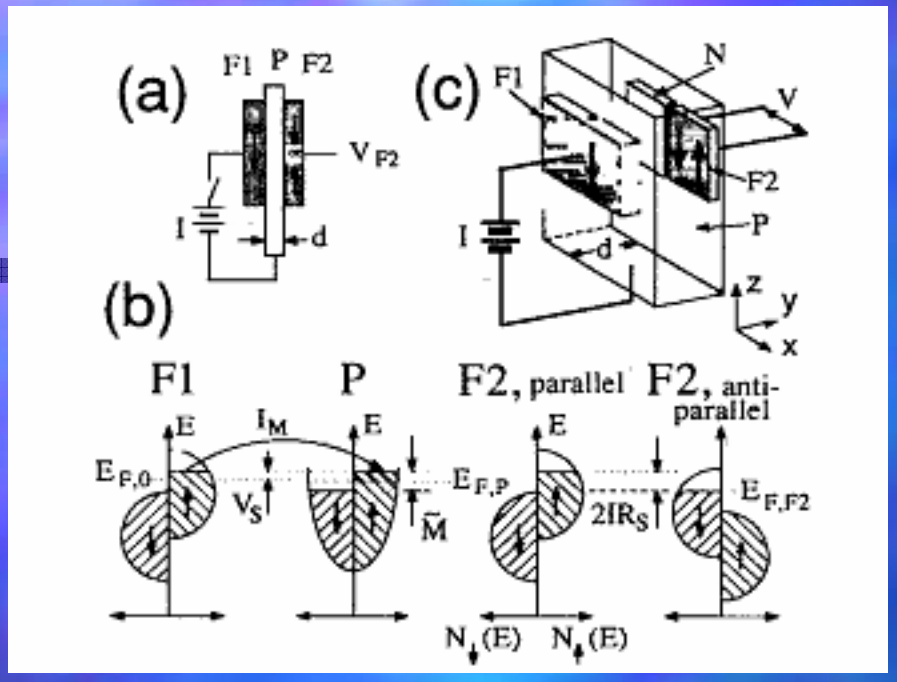

(a) Pedagogical model of three terminal device. Arrows in F_1 and F_2 refer to magnetization orientation as determined by majority spin subband. (b) Diagrams of the densities of state, N(E), of the ferromagnet paramagnet ferromagnet system depicted in (a). (c) The geometry used to measure $V_{F2.}$ P is depicted transparent.

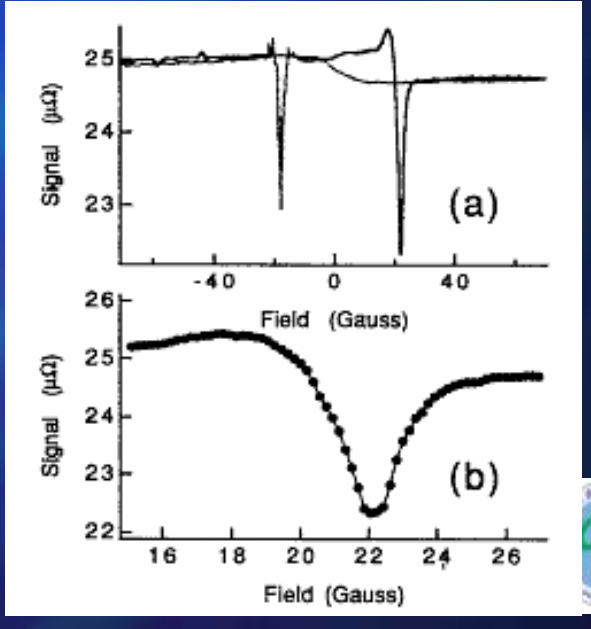

d=1.6μm, I=4mA

M. Johnson, PRL **70**, 2142 (1993)

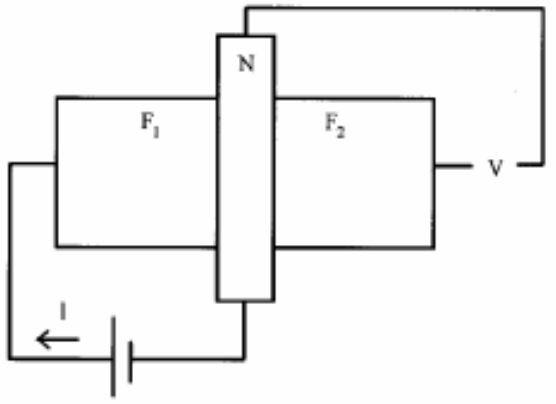

FIG. 1. Schematic drawing of Johnson's spin switch device. The voltage measured as shown depends on the relative orientation of the magnetizations in F_1 and F_2.

$$\mu_{\pm}(z) = -e\rho_F^*(1-\beta^2)\frac{J}{2}(z+a) + e\rho_N^*\frac{J}{2}a + \delta\mu^{F_1} + \Delta\mu_{\pm}^{F_1}(z) \quad \text{in } F_1,$$

$$\mu_{\pm}(z) = -e\rho_N^*\frac{J}{2}z + \Delta\mu_{\pm}^{N}(z) \quad \text{in } N,$$

由波茲曼方程式出發，可以在理論上探討產生訊號與各物理量之間的關係。 進一步可由實驗證實如何能得到最大訊號。

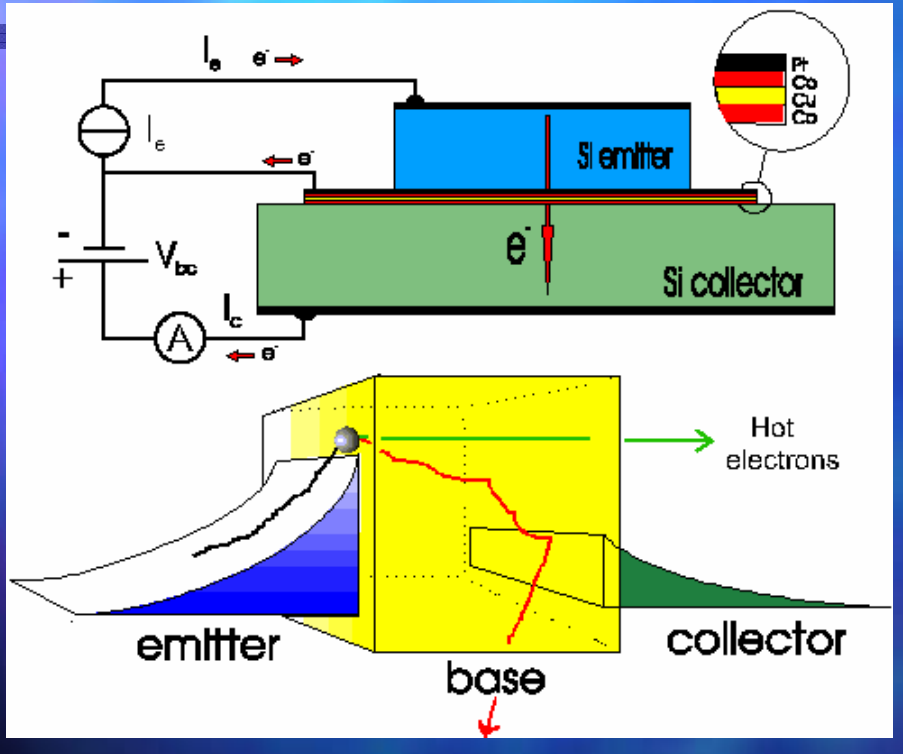

Schematic cross-section of the spin-valve transistor. A Co/Cu/CO sandwich base is sputtered on a silicon substrate. Vacuum bonding is done while sputtering the Pt layer.
The picture shows the band-structure of the spin-valve transistor

Monsma et al, PRL **74,** 5260 (1995)

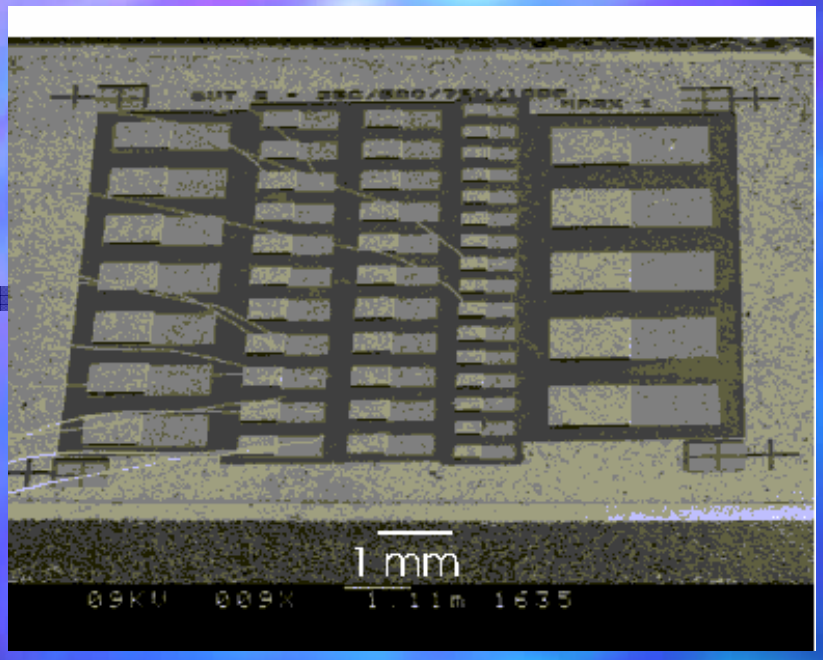

A scanning electron microscope photo of several vacuum bonded and fully processed Si-Co-Cu-Co-Pt-Si spin-valve transistors.

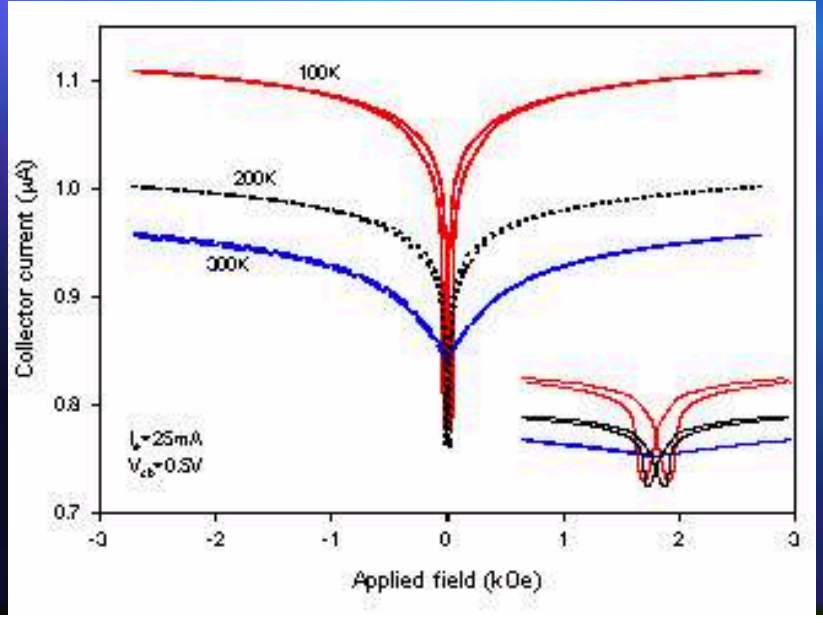

Collector current variation versus magnet field at a emitter current of 25mA, temperature 100, 200 and 300K, range from -240 to 240 kA/m. The inset on the left-hand side accentuates the small field behavior from -24 to 24kA/m

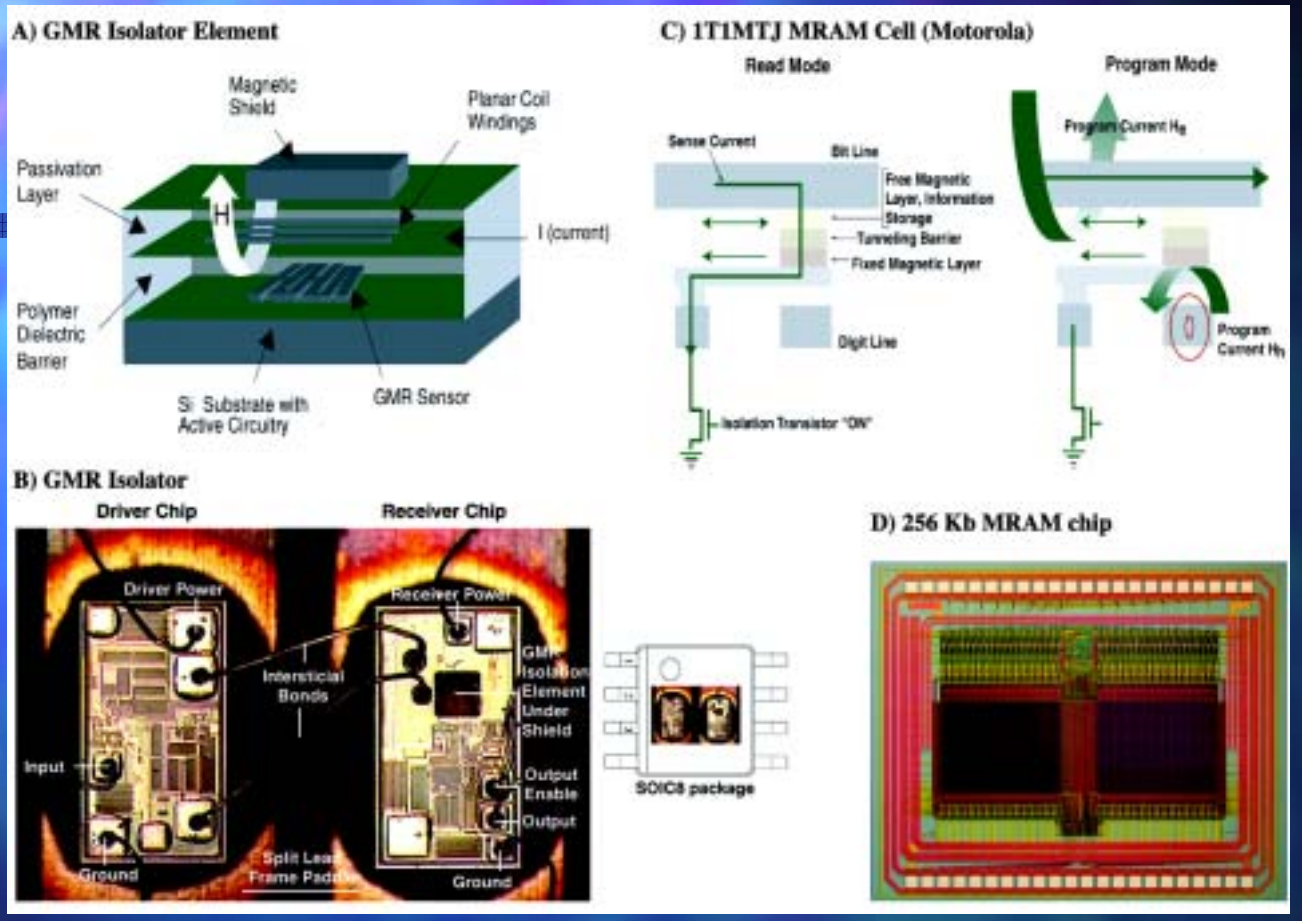

Device applications. (B) courtesy of NVE; (D) courtesy of Motorola

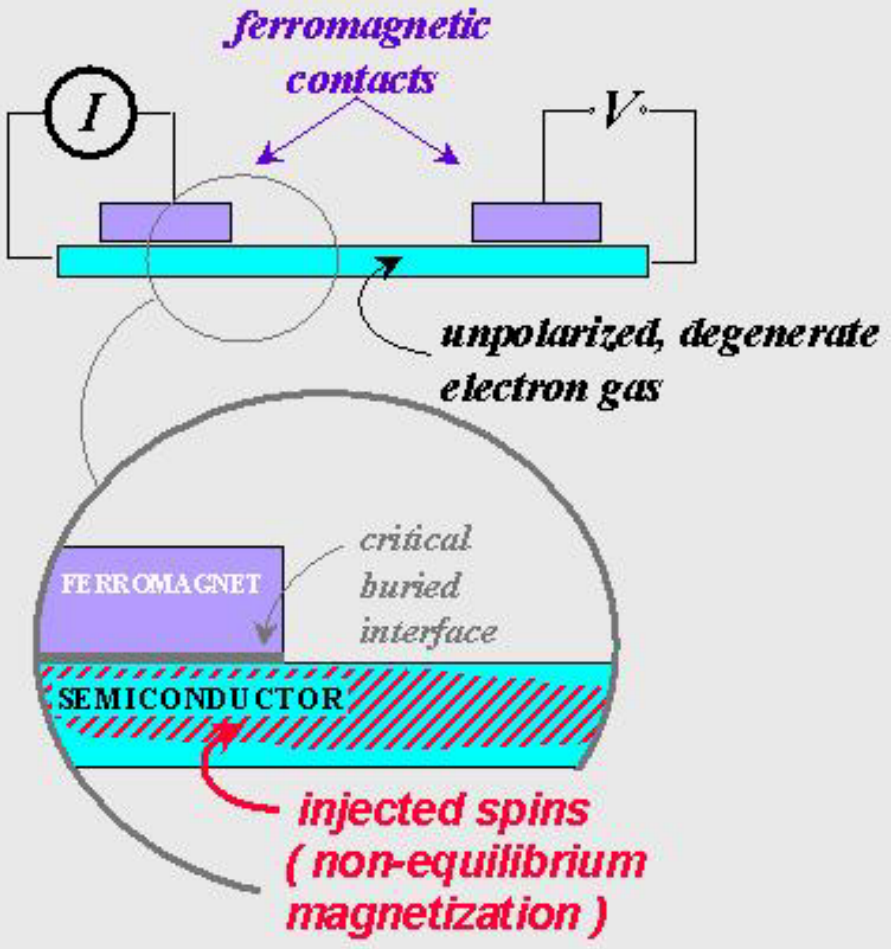

From Roukes et al, Caltech

- Major advantage to using InAs instead of GaAs is that unalloyed metal contacts can be made directly to InAs.

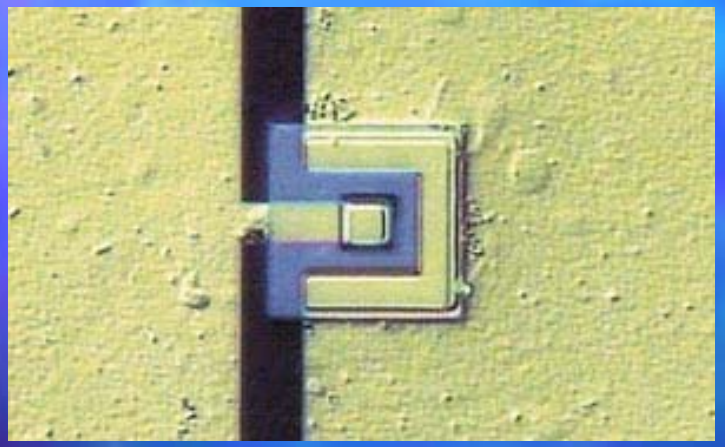

From IMEC

Vertical spin transistors are fabricated by sandwiching a metallic "spin valve" base between a gallium arsenide emitter and a silicon collector. These stacks are created by wafer bonding in ultrahigh vacuum, while the metallic base layers are built up by thin-film techniques. IMEC researchers have also experimented with alternative fabrication routes, such as growing epitaxial magnetic semiconductor structures by depositing semiconductors and magnetic metals in a molecular beam epitaxy system.

Another device investigated by SPIDER is the lateral spin transistor – a magnetic version of a field-effect transistor. This device is fabricated by placing two magnetic contacts, the source and drain, on a semiconductor channel. A spin-polarized current flows between the source and drain, and the drain current can be modulated by changing the magnetization of the source and drain electrodes.

Y. Ohno et al, Nature 402, 790 (1999)

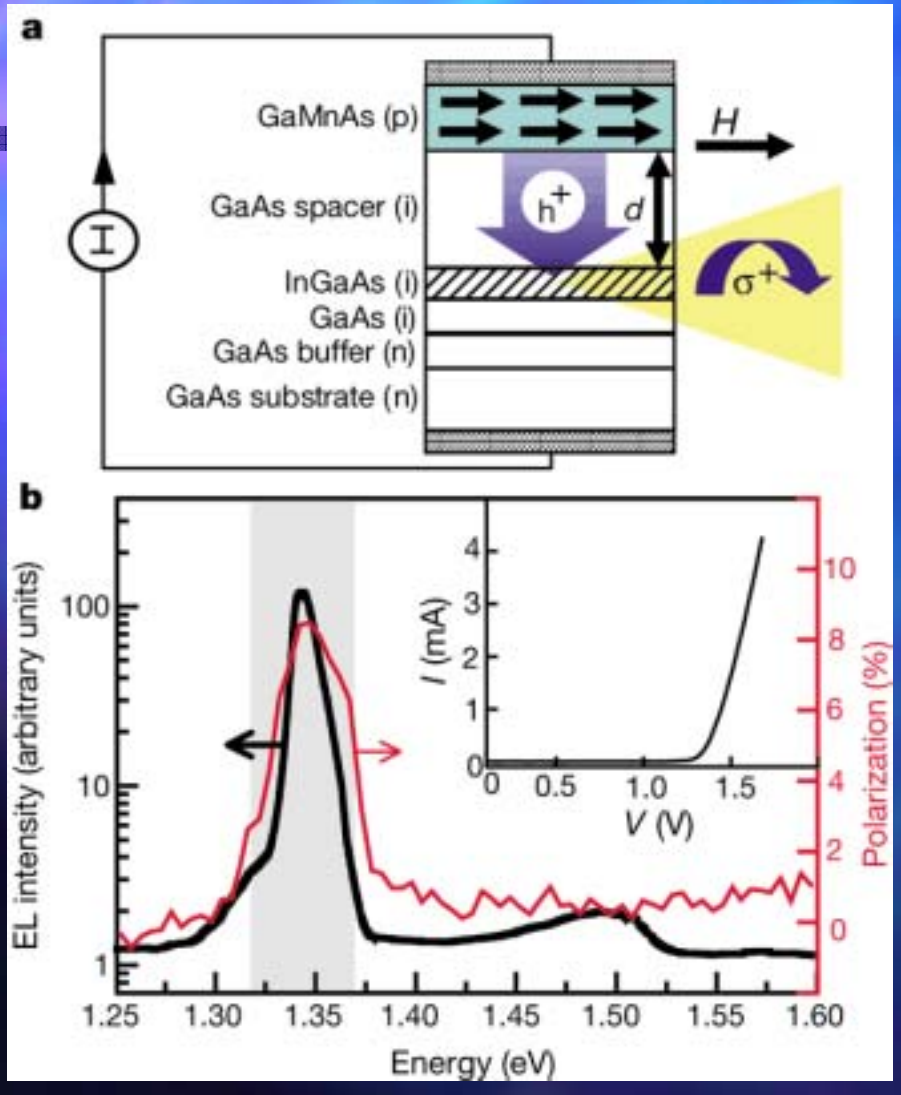

Electrical spin injection in an epitaxially grown ferromagnetic semiconductor heterostructure, based on GaAs. a, Spontaneous magnitization develops below the Curie temperature T_C in the ferromagnetic p-type semiconductor (Ga,Mn)As, depicted by the black arrows in the green layer. Under forward bias, spin-polarized holes from (Ga,Mn)As and unpolarized electrons from the n-type GaAs substrate are injected into the (In,Ga)As quantum well (QW, hatched region), through a spacer layer with thickness d, producing polarized EL. b, Total electroluminescence (EL) intensity of the device (d = 20 nm) under forward bias at temperature T = 6 K and magnetic field H = 1,000 Oe is shown (black curve) with its corresponding polarization (red curve). Current I = 1.43 mA. Note that the polarization is largest at the QW ground state (E = 1.34 eV). The EL and polarization are plotted on semi-log and linear scales, respectively. Inset, a current–voltage plot characteristic of a 20-nm spacer layer device..

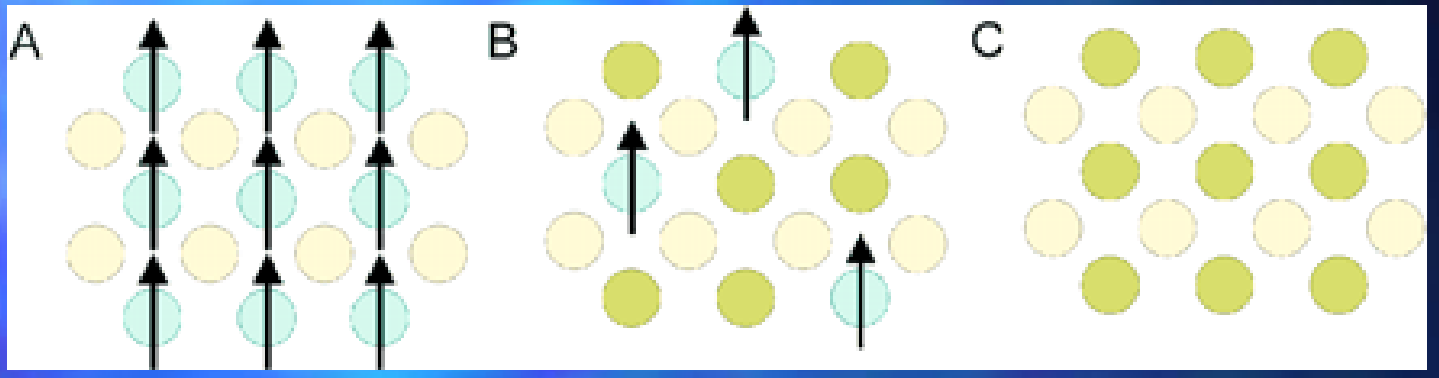

Three types of semiconductors: (A) a magnetic semiconductor, in which a periodic array of magnetic element is present; (B) a diluted magnetic semiconductor, an alloy between nonmagnetic semiconductor and magnetic element; and (C) a nonmagnetic semiconductor, which contains no magnetic ions. (From Ohno, Science 281, 951 (1998).)

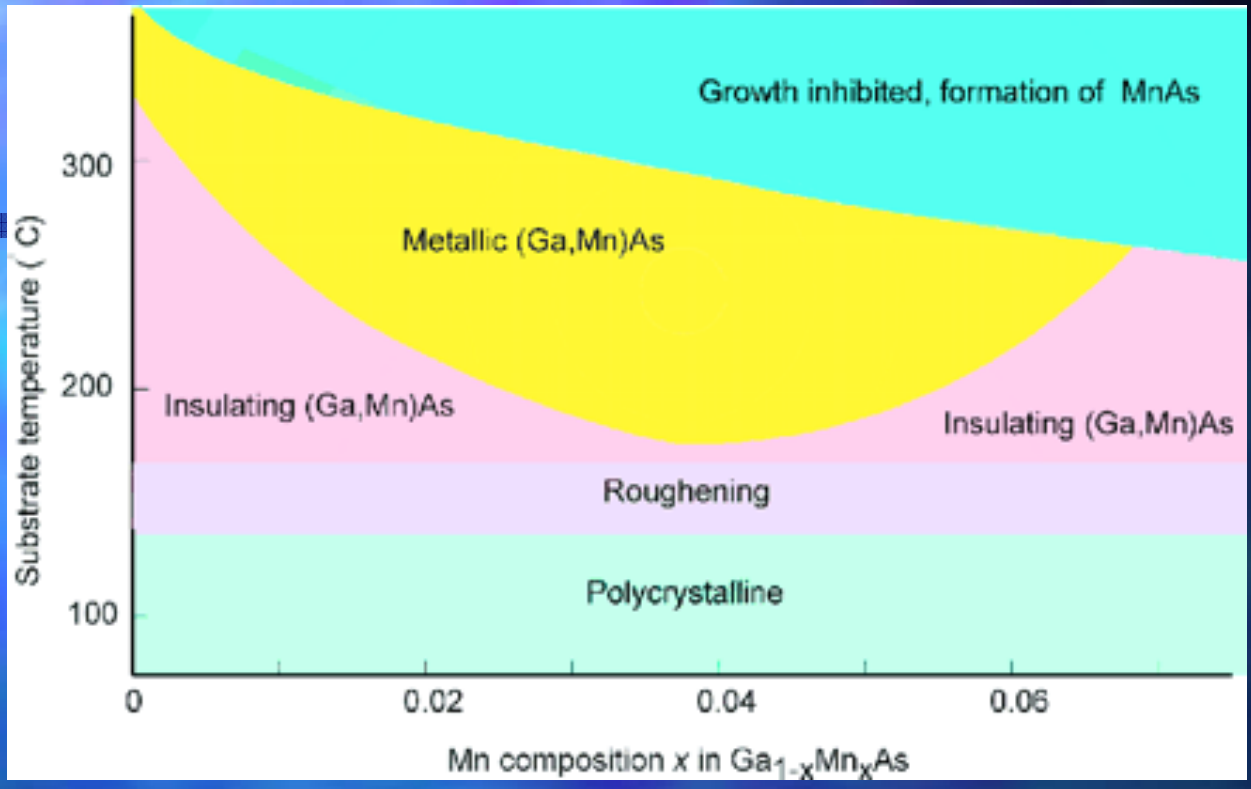

Schematic phase diagram showing the relation between growth parameters (substrate temperature and Mn concentration) and the properties of (Ga,Mn)As grown by molecular beam epitaxy. The high concentration of Mn in excess of its solubility limit was introduced by nonequilibrium growth at low temperatures. (From Ohno, Science 281, 951 (1998).)

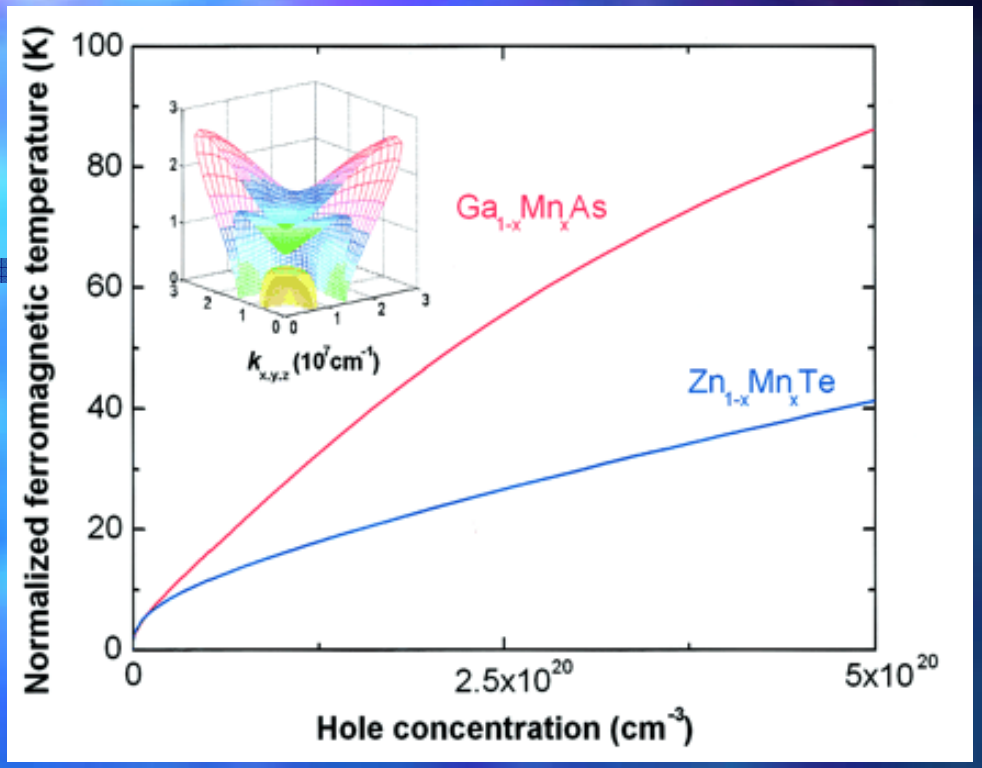

Normalized ferromagnetic temperature T_F^{nor} as a function of hole concentration. Inset shows an example of the cross section of the Fermi volume of holes in a ferromagnetic zinc-blende semiconductor: Nonzero magnetization leads to a splitting of the valence band into four subbands. This complex valence-band structure was used to determine the mean-field values of T_F^{nor} for p-$Ga_{0.95}Mn_{0.05}As$ and p-$Zn_{0.95}Mn_{0.05}Te$ (solid lines) and to establish the chemical trends. (From Dietl et al, Science 287, 1019 (2000).)

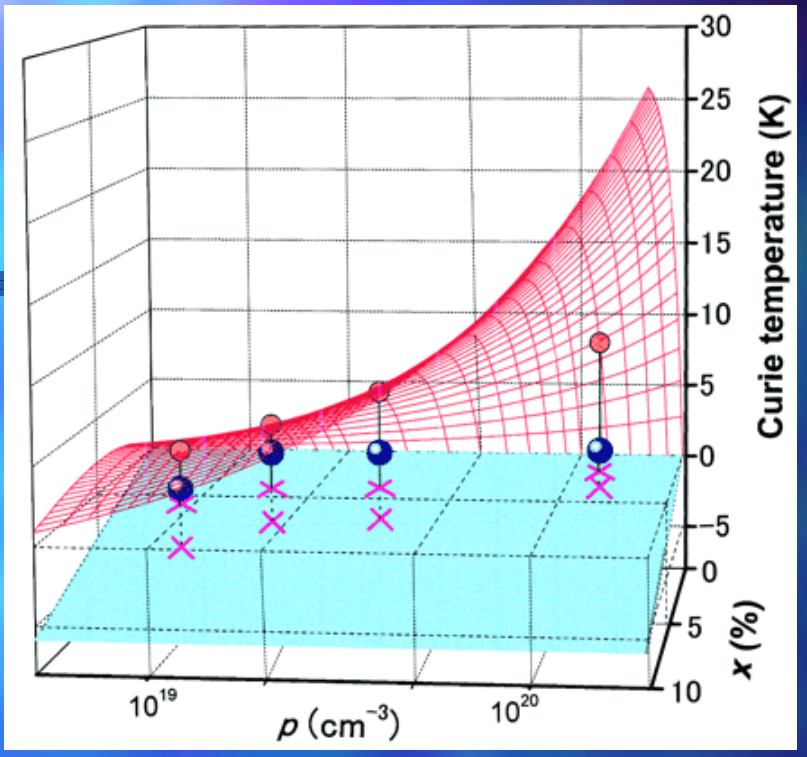

Curie temperature T_C in Zn_{1-x} Mn_xTe:N for various Mn contents x and hole concentrations p deduced from the Hall resistance at 300 K. The plane with upper crosses corresponds to $T_C = 0$. Experimental values are marked by blue spheres (22) and theoretical predictions by the red mesh and attached yellow spheres. T_C is determined by a competition between the hole-induced ferromagnetic interactions (characterized by T_F^{nor}) and the antiferromagnetic interactions, described by T_{AF}, shown by the plane with lower crosses. (From Dietl et al, Science 287, 1019 (2000).)

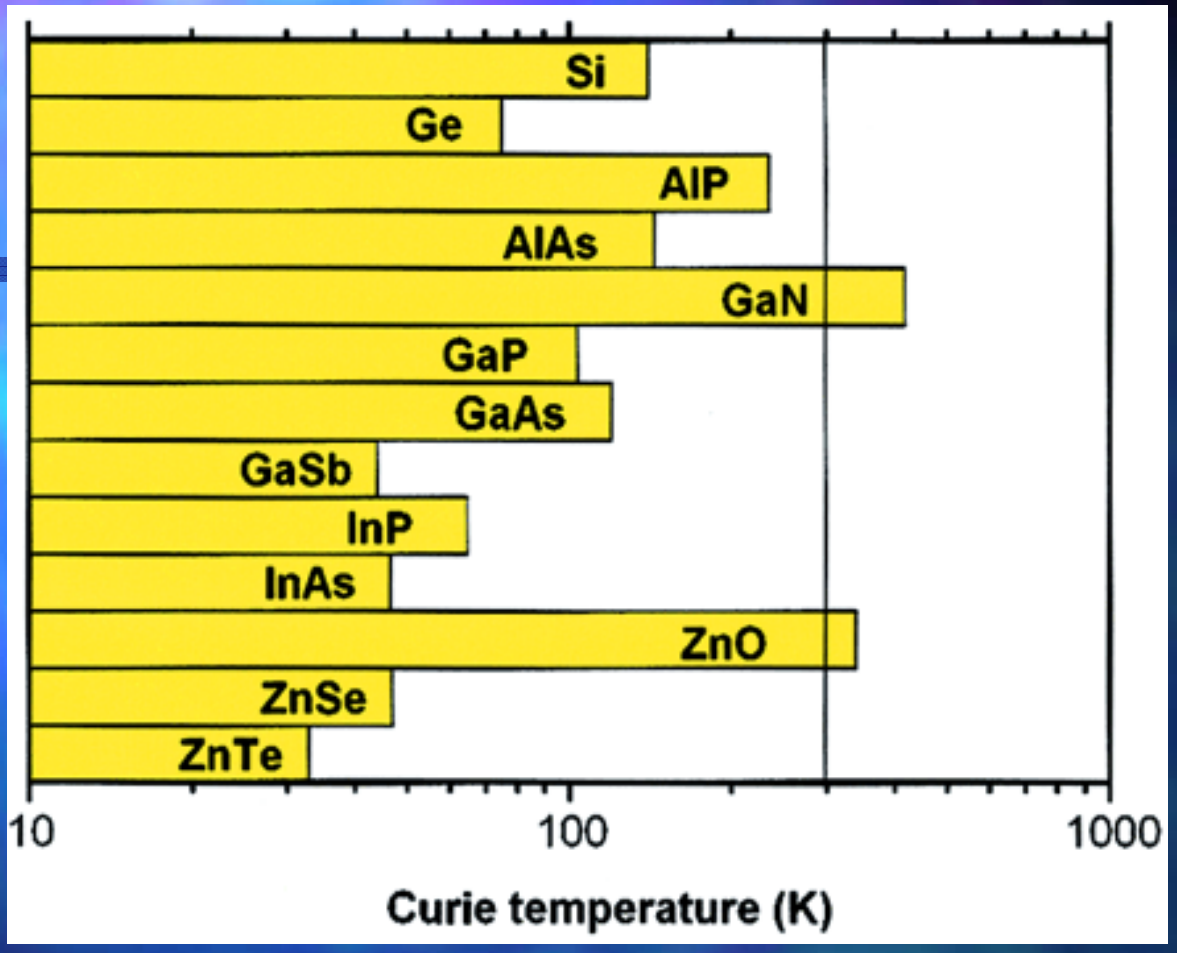

Computed values of the Curie temperature T_C for various p-type semiconductors containing 5% of Mn and 3.5×10^{20} holes per cm^3.

BACKGROUND

A. Giant Magnetoresistance (Disc. 1988)

Change Magnetic Order → Change Resistance (or Current)

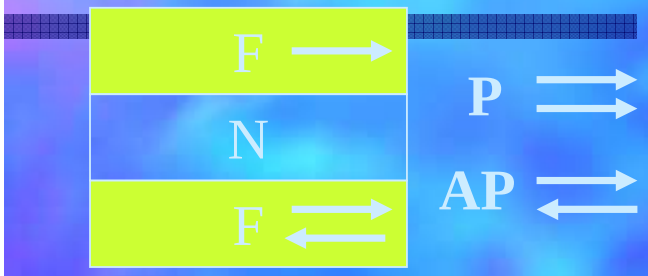

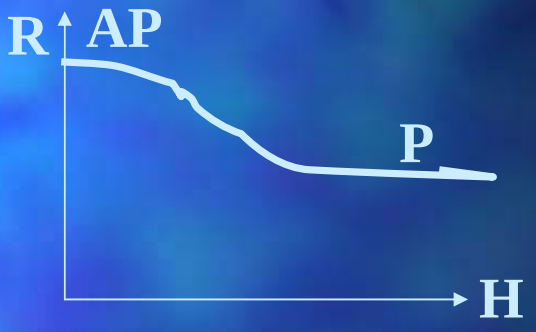

Read Heads; Sensors; MRAM (Tunneling)

B. Current-Driven Switching =’Inverse’ Effect. (Pred. 1996)

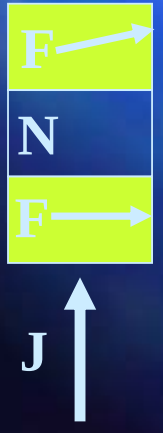

First F Polarizes J. Polarized J exerts Torque on second F. $+J_c$ Flips to AP; $-J_c$ Flips to P.

Write in MRAM? Write on MR Media?

Q: Physics; Minimize J_c

- Current-driven magnetization reversal

INITIAL THEORY

1996-1998: Berger and Slonczewski predict

High-Current-Density-Induced:

(a) **Coherent Spin-Wave Generation**, and

(b) **Magnetization Reversal**

PHYSICS

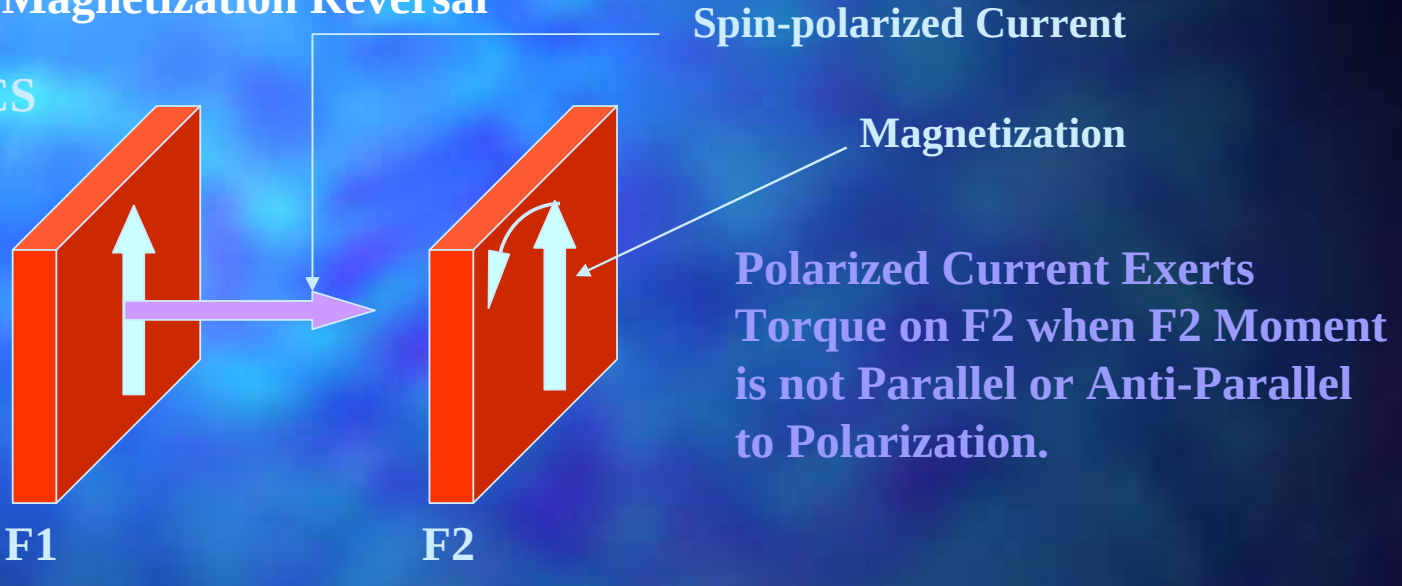

Polarized Current Exerts Torque on F2 when F2 Moment is not Parallel or Anti-Parallel to Polarization.

FIRST EXPERIMENTS

1998 (PRL), 2000 (Nature): MSU + Grenoble

Coherent Spin-Wave Generation?.

1999-2002 (PRL & Science): Cornell.

Layer Magnetization Reversal.

V vs I, R = V/I vs I, and dV/dI vs I (+ small ac current).

A: Hysteretic = Non-Reversible

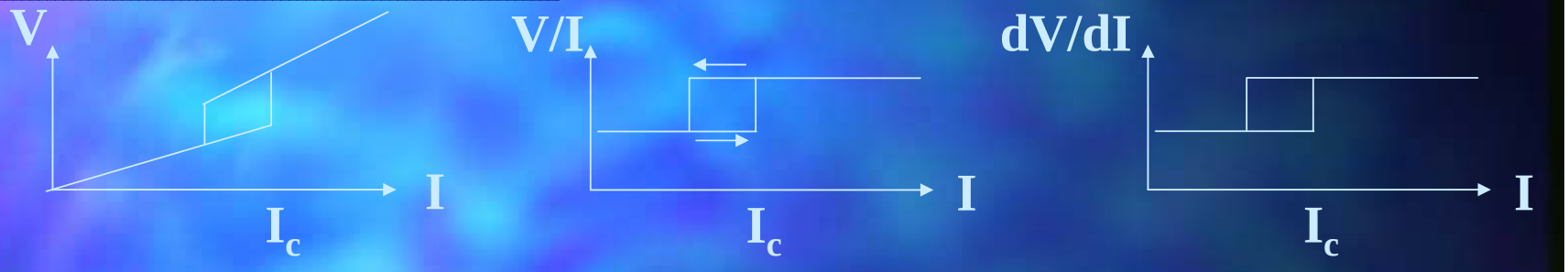

B: Non-Hysteretic = Reversible